Protein kinase CK2 contributes to the organization of sodium channels in axonal membranes by regulating their interactions with ankyrin G

Aline Brechet, Marie Fache, Anna Brachet, Géraldine Ferracci, Agnès Baude, Marie Irondelle, Sandrine Pereira, Christophe Leterrier, Bénédicte Dargent

Published December 8, 2008

Protein kinase CK2 contributes to the organization of sodium channels in axonal membranes by regulating their interactions with ankyrin G

Aline Bréchet,[1,2] Marie-Pierre Fache,[1,2] Anna Brachet,[1,2] Géraldine Ferracci,[2,4] Agnés Baude,[3] Marie Irondelle,[1,2] Sandrine Pereira,[1,2] Christophe Leterrier,[1,2] and Bénédicte Dargent[1,2]

[1]Institut National de la Santé et de la Recherche Médicale, Unité Mixte de Recherche 641, Marseille F-13916, France
[2]Université de la Méditerranée, Faculté de Médecine Secteur-Nord, Institut Fédératif de Recherche 11, Marseille F-13916, France
[3]Université de la Méditerranée, Centre National de la Recherche Scientifique, Unité Mixte de Recherche 6231, Marseille F-13916, France
[4]Centre d'Analyse Protéomique de Marseille, Marseille F-13916, France

In neurons, generation and propagation of action potentials requires the precise accumulation of sodium channels at the axonal initial segment (AIS) and in the nodes of Ranvier through ankyrin G scaffolding. We found that the ankyrin-binding motif of $Na_v1.2$ that determines channel concentration at the AIS depends on a glutamate residue (E1111), but also on several serine residues (S1112, S1124, and S1126). We showed that phosphorylation of these residues by protein kinase CK2 (CK2) regulates Na_v channel interaction with ankyrins. Furthermore, we observed that CK2 is highly enriched at the AIS and the nodes of Ranvier in vivo. An ion channel chimera containing the $Na_v1.2$ ankyrin-binding motif perturbed endogenous sodium channel accumulation at the AIS, whereas phosphorylation-deficient chimeras did not. Finally, inhibition of CK2 activity reduced sodium channel accumulation at the AIS of neurons. In conclusion, CK2 contributes to sodium channel organization by regulating their interaction with ankyrin G.

Introduction

In neurons, action potentials are generated at the axonal initial segment (AIS), and in myelinated axons, their saltatory conduction occurs via the nodes of Ranvier (Stuart et al., 1997; Kole et al., 2008). These processes require a precise distribution of voltage-gated sodium channels that accumulate at high density in these two highly specialized axonal subdomains, defined by the segregation of the cytoskeletal adaptor complex ankyrin G/βIV spectrin (Zhou et al., 1998; for review see Salzer, 2003). This scaffolding complex not only concentrates voltage-gated sodium channels $Na_v1.2$ and $Na_v1.6$ (Boiko et al., 2003), but also potassium channels KCNQ2/KCNQ3 (Devaux et al., 2004; Pan et al., 2006), cell adhesion molecules neurofascin-186 (NF-186), and neuronal cell adhesion molecule (NrCAM; Davis et al., 1996; Basak et al., 2007; Dzhashiashvili et al., 2007; Hedstrom et al., 2007). Recently, several additional new components have been shown to accumulate at the AIS and nodes, such as members of the nuclear factor κB signaling pathway (Schultz et al., 2006; Politi et al., 2007), growth factors FHF2 and FHF4 (Lou et al., 2005; Wittmack et al., 2004), and extracellular matrix components aggrecan and brevican (Bruckner et al., 2006; John et al., 2006). The implications of these newly characterized components in AIS and node assembly, maintenance, or function are still unknown.

Although they share a common subset of proteins, the assembly of AIS and nodes of Ranvier has been shown to differ (Dzhashiashvili et al., 2007). The formation of the AIS depends on intrinsic properties of the neuron and occurs during the early steps in establishment of neuronal polarity in cultured neurons (Alessandri-Haber et al., 1999; Boiko et al., 2007; Yang et al., 2007). Genetic, biochemical, and cell biology studies converge on the crucial role of ankyrin G as the key player in organizing the AIS (Zhou et al., 1998; Jenkins and Bennett, 2001; Dzhashiashvili et al., 2007; Hedstrom et al., 2007). Unlike the AIS, the formation of the nodes of Ranvier requires exquisite communication with

Correspondence to Bénédicte Dargent: benedicte.dargent@univmed.fr

Sandrine Pereira's present address is Institut National de la Santé et de la Recherche Médicale, Unité Mixte de Recherche 910, Université de la Méditerranée, Faculté de Médecine secteur-Timone, Marseille 13385, France.

Abbreviations used in this paper: AIS, axonal initial segment; CK2, protein kinase CK2; CNS, central nervous system; DIV, days in vitro; DMAT, 2-dimethylamino-4,5,6,7-tetrabromo1*H*-benzimidazole; MAP2, microtubule-associated protein 2; MBD, membrane-binding domain; MBD-ank, MBD-ankyrin; PNS, peripheral nervous system; SPR, surface plasmon resonance.

The Rockefeller University Press $30.00
J. Cell Biol. Vol. 183 No. 6 1101–1114
www.jcb.org/cgi/doi/10.1083/jcb.200805169

Published December 8, 2008

myelinating cells. In the nodes of the peripheral nervous system (PNS), the aggregation of axonal components is dependent on ankyrin G, but the priming event is initiated by gliomedin, a membrane protein positioned in the microvilli of the Schwann cell facing the node of Ranvier, via a direct interaction with the extracellular domain of neurofascin-186 and neuronal cell adhesion molecule (Eshed et al., 2005, 2007; Dzhashiashvili et al., 2007). The nucleation of cell adhesion molecules in turn induces ankyrin G, βIV spectrin, and sodium channel recruitment (Eshed et al., 2005; Dzhashiashvili et al., 2007).

Among the interactions responsible for AIS formation and maintenance, the Na_v sodium channel interaction with ankyrin G is of particular importance (Lambert et al., 1997; Zhou et al., 1998; Garrido et al., 2003; Lemaillet et al., 2003; Fache et al., 2004). To circumvent difficulties in expressing full-length Na_v in hippocampal neurons, we previously developed an approach based on CD4 chimera expression (Garrido et al., 2001). This approach allowed us to identify a sequence of 27 residues, called the AIS motif, that determines sodium channel targeting and clustering at the AIS (Garrido et al., 2003; Fache et al., 2004). This conserved determinant, located in the cytoplasmic linker between domains II and III of the Na_v1 pore-forming α subunit (Na_v1 II-III), constitutes the ankyrin-binding motif of Na_v sodium channels. We also showed that the mutation of the glutamate residue $Na_v1.2$ E1111 was sufficient to impair the compartmentalization at the AIS of CD4–$Na_v1.2$ II-III, a chimera in which the cytoplasmic region of CD4 was replaced by $Na_v1.2$ II-III (Fache et al., 2004). In the meantime, an independent study demonstrated that the PIALGESD sequence located within the AIS motif directly interacts with the membrane-binding domain (MBD; Lemaillet et al., 2003), a domain highly conserved in ankyrin G and ankyrin B (Kordeli et al., 1995). Ankyrin G and B display a complementary subcellular distribution in the axons of cultured hippocampal neurons (Boiko et al., 2007) and in myelinated fibers (Kordeli et al., 1990; Bennett and Lambert, 1999; Ogawa et al., 2006). Strikingly, sodium channel accumulation is restricted to ankyrin G–positive subdomains both in vivo and in cultured neurons (Boiko et al., 2001, 2003). Because the ankyrin-binding motif is highly conserved in all neuronal sodium channels (Garrido et al., 2003; Lemaillet et al., 2003; Pan et al., 2006) and binds to a domain highly conserved in ankyrin B and ankyrin G (Kordeli et al., 1995), it is difficult to understand how sodium channels are specifically restricted to ankyrin G–positive subdomains in the axon. We thus addressed the question as to whether an additional mechanism specifies sodium channel accumulation at the AIS and in the nodes of Ranvier.

To further analyze the molecular mechanisms involved in the discrete localization of sodium channels in the axonal membrane, we chose to use $K_v2.1$-$Na_v1.2$, an ion channel chimera in which the C terminus of the $K_v2.1$ potassium channel was replaced by the AIS motif of $Na_v1.2$ instead of CD4–$Na_v1.2$ II-III (Garrido et al., 2003; Fache et al., 2004). We have previously shown that endocytosis and domain-selective tethering confers CD4-$Na_v1.2$ II-III segregation at the AIS (Fache et al., 2004). However, the endocytotic signal identified in the $Na_v1.2$ II-III linker (Fache et al., 2004) is not present in $K_v2.1$-Na_v1, which suggests that it could follow a different trafficking pathway and be directly sorted to the AIS. Therefore, we first determined the critical residues of the ankyrin-binding motif responsible for $K_v2.1$-$Na_v1.2$ accumulation at the AIS. We observed that segregation was driven by the joint action of two types of residue: a glutamate residue ($Na_v1.2$ E1111) and several serine residues ($Na_v1.2$ S1112, S1123, S1124, and S1126). Sequence analysis reveals that these serine residues are part of potential protein kinase CK2 (CK2) phosphorylation sites. Using the surface plasmon resonance (SPR) method (Wilson, 2002; Rich and Myszka, 2007), we directly demonstrated that CK2-mediated phosphorylation regulates the interaction between the Na_v1 ankyrin-binding motif and the MBD of axonal ankyrins. Furthermore, a high concentration of CK2 in the AIS and the nodes of Ranvier was detected in vivo and in hippocampal cultures, which is consistent with a possible role of CK2 in regulating the interaction between Na_v and ankyrin. Moreover, a peculiar property of the $K_v2.1$-$Na_v1.2$ chimera allowed us to unravel the functional significance of this regulation: expression of the $K_v2.1$-$Na_v1.2$ chimera containing the ankyrin-binding motif of $Na_v1.2$-depleted endogenous sodium channels in the AIS of cultured hippocampal neurons. In contrast, chimeras containing a phosphorylation-deficient ankyrin-binding motif failed to perturb sodium channel accumulation at the AIS. Finally, inhibition of CK2 reduced sodium channel concentration at the AIS of cultured neurons. Altogether, our findings are consistent with the conclusion that CK2 contributes to the accumulation of sodium channels at the AIS and in the nodes of Ranvier by regulating their interaction with ankyrin G.

Results

Abrogation of the glutamate residue of the Na_v1 ankyrin-binding motif is not sufficient to impair ion channel segregation at the AIS

When expressed by transfection in cultured hippocampal neurons, the potassium channel $K_v2.1$ was clustered at the cell surface on soma and on proximal dendrites identified by microtubule-associated protein 2 (MAP2) staining (Fig. 1 A), as described previously (Lim et al., 2000). The deletion of the C terminus of $K_v2.1$ ($K_v2.1$-ΔCter) induced a loss of compartmentalization (Fig. 1 B). The addition of a segment encompassing the AIS motif of sodium channel $Na_v1.2$ (amino acids 1,080–1,203) to the C terminus of $K_v2.1$ ($K_v2.1$-$Na_v1.2$) was sufficient to redirect $K_v2.1$ to the AIS (Fig. 1 C). This was observed at the cell surface of 70.9 ± 10.9% (n = 609) of cells expressing $K_v2.1$-$Na_v1.2$, in line with our previous study (Garrido et al., 2003). To determine the critical residues involved in $K_v2.1$-$Na_v1.2$ segregation, we first converted $Na_v1.2$ E1111 into alanine, a point mutation that was sufficient to impair CD4-$Na_v1.2$ II-III compartmentalization at the AIS (Fache et al., 2004). Because a mutation of the corresponding E residue ($Na_v1.5$ E1053K) altered the trafficking of sodium channel $Na_v1.5$ in cardiomyocytes (Mohler et al., 2004), we differentially stained the surface and total channel populations. Surface staining was observed in 58.3% (n = 230) of the cells expressing the $K_v2.1$-$Na_v1.2$ E1111A mutant and in 90.4% (n = 240) of the cells expressing $K_v2.1$-$Na_v1.2$. Strikingly, $K_v2.1$-$Na_v1.2$ E1111A was correctly localized at the AIS in 52.7 ± 13.9% (n = 178) of the cells displaying surface

Supplemental Material can be found at:
http://jcb.rupress.org/cgi/content/full/jcb.200805169/DC1

Published December 8, 2008

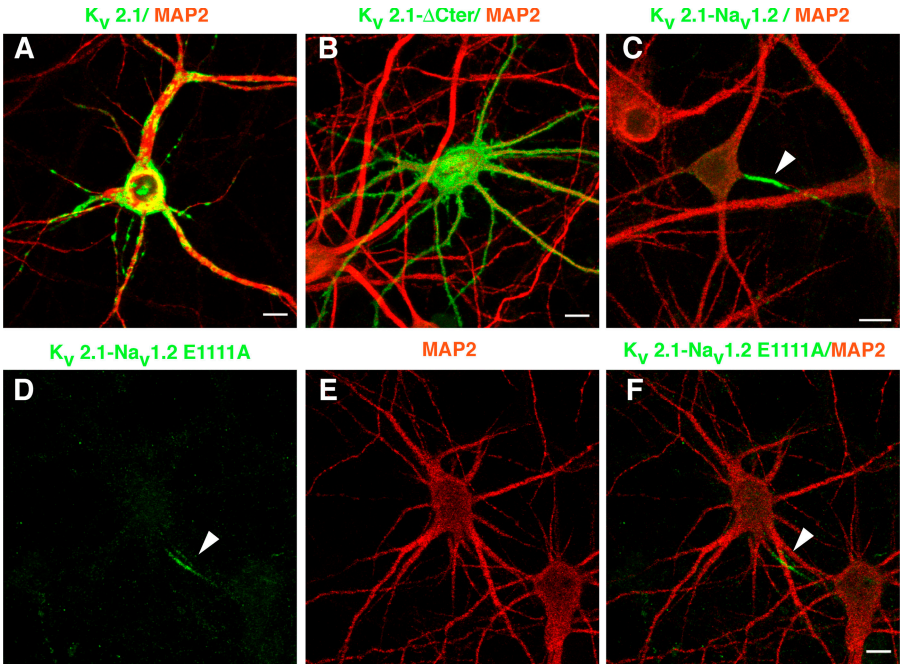

Figure 1. **Abrogation of E1111 of the Na_v1.2 ankyrin-binding motif did not impair ion channel segregation at the AIS of hippocampal neurons.** Cell surface distribution of K_v2.1 (A), K_v2.1-ΔCter (B), K_v2.1-Na_v1.2 (C), and K_v2.1-Na_v1.2 E1111A mutant (D–F) in cultured hippocampal neurons. The addition of the Na_v1.2 ankyrin-binding motif to the C terminus of K_v2.1-ΔCter segregated K_v2.1 at the AIS (C, arrow). K_v2.1-Na_v1.2 compartmentalization at the AIS was not impaired by the Na_v1.2 E1111A mutation (D and F, arrow). The indicated constructs were immunodetected with an antibody to myc (green) before cell permeabilization; the somatodendritic domain was subsequently identified by MAP2 staining. Bars, 10 μm.

staining (Fig. 1, D–F, and Fig. 2 E). After cell permeabilization, this mutant was visualized not only in the soma and throughout the dendrites but also in the ER identified by calreticulin costaining (unpublished data). In contrast, K_v2.1-Na_v1.2 was only occasionally detected in the ER (unpublished data). These findings indicate that the abrogation of Na_v1.2 E1111 altered K_v2.1-Na_v1.2 trafficking, presumably by favoring retention in the ER, but did not impair its ability to be targeted to the AIS. In view of these observations, we surmised that, in addition to E1111, other residues of the ankyrin-binding motif contribute to K_v2.1-Na_v1.2 segregation at the AIS.

A combination of glutamate and serine residues is required for channel segregation at the AIS

Sequence analysis of the targeting and clustering motif of Na_v1.2 (Blom et al., 2004) revealed that S1112, S1124, and S1126 contribute to three potential phosphorylation sites for CK2, defined by the sequence S/TXXD/E (Meggio and Pinna, 2003). S1123 could also be phosphorylated by CK2 after phosphorylation of S1126 (Meggio and Pinna, 2003). All these serine residues are highly conserved in the sodium channel types (Na_v1.1-1.3 and Na_v1.6) predominantly expressed in the central nervous system (CNS; Fig. 2 A). In an attempt to identify the additional residues involved in K_v2.1-Na_v1.2 segregation at the AIS, we thus evaluated the impact of different serine mutations (S1112A; S1123-24A; S1126A; S1123-24-26A, designated 3SA; and S1112-23-24-26A, designated 4SA; Fig. 2 C) on the steady-state surface distribution of K_v2.1-Na_v1.2 in hippocampal neurons. All K_v2.1-Na_v1.2 serine mutants were predominantly compartmentalized at the AIS, whatever the number of serine mutations (Fig. 2, B and C). In contrast, serine mutations associated with the E1111A mutation profoundly perturbed K_v2.1-Na_v1.2 compartmentalization (Fig. 2, D and E). In fact, segregation was totally impaired by combining E1111A with either S1126A or S1123-24A mutations (Fig. 2, D and E). Mutations E1111A-S1112A significantly increased the number of cells with a nonpolarized distribution of K_v2.1-Na_v1.2 (Fig. 2 E). These results indicated that K_v2.1-Na_v1.2 segregation is dependent on the concerted action of E1111 with serine residues (S1112, S1123-24, or S1126).

The interaction between neuronal sodium channels and axonal ankyrins is regulated by CK2 phosphorylation

The ankyrin-binding motif of sodium channels directly interacts with a highly conserved domain in ankyrin G and B called the MBD (Srinivasan et al., 1992; Lemaillet et al., 2003; Mohler et al., 2004). We next examined the possibility that CK2-mediated phosphorylation regulates this interaction. We first determined whether the ankyrin-binding motif of Na_v1.2 is phosphorylated by CK2 by conducting in vitro phosphorylation assays with GST proteins fused either to the linker II-III of Na_v1.2 (Na_v1.2 II-III) or truncated mutants (Fig. 3 A). In the presence of CK2, Na_v1.2 II-III was phosphorylated in vitro, as visualized by autoradiography (Fig. 3 B). A similar result was obtained when the C terminus of the Na_v1.2 II-III construct was truncated at residue 1133, whereas the deletion of the AIS motif (GST-Na_v1.2 989–1,079) resulted in a loss of signal. A positive signal was observed with a GST protein bearing the segment encompassing the AIS motif (GST-Na_v1.2 1,080–1,203). Several site-directed mutations of GST-Na_v1.2 1,080–1,203 were generated. The respective abrogation of S1112, S1123, or S1124 did not affect in vitro phosphorylation of GST-Na_v1.2 1,080–1,203 by CK2 (Fig. 3 C). In contrast, S1126A mutation and the double mutation S1123-24A resulted in a decrease in signal. The double mutation (S1124-26A) and the triple mutation (S1112-24-26A) impaired GST-Na_v1.2 1,080–1,203 phosphorylation (Fig. 3 C). All together, these results indicated that the ankyrin-binding motif of Na_v1.2 is phosphorylated in vitro by CK2. We next examined

Published December 8, 2008

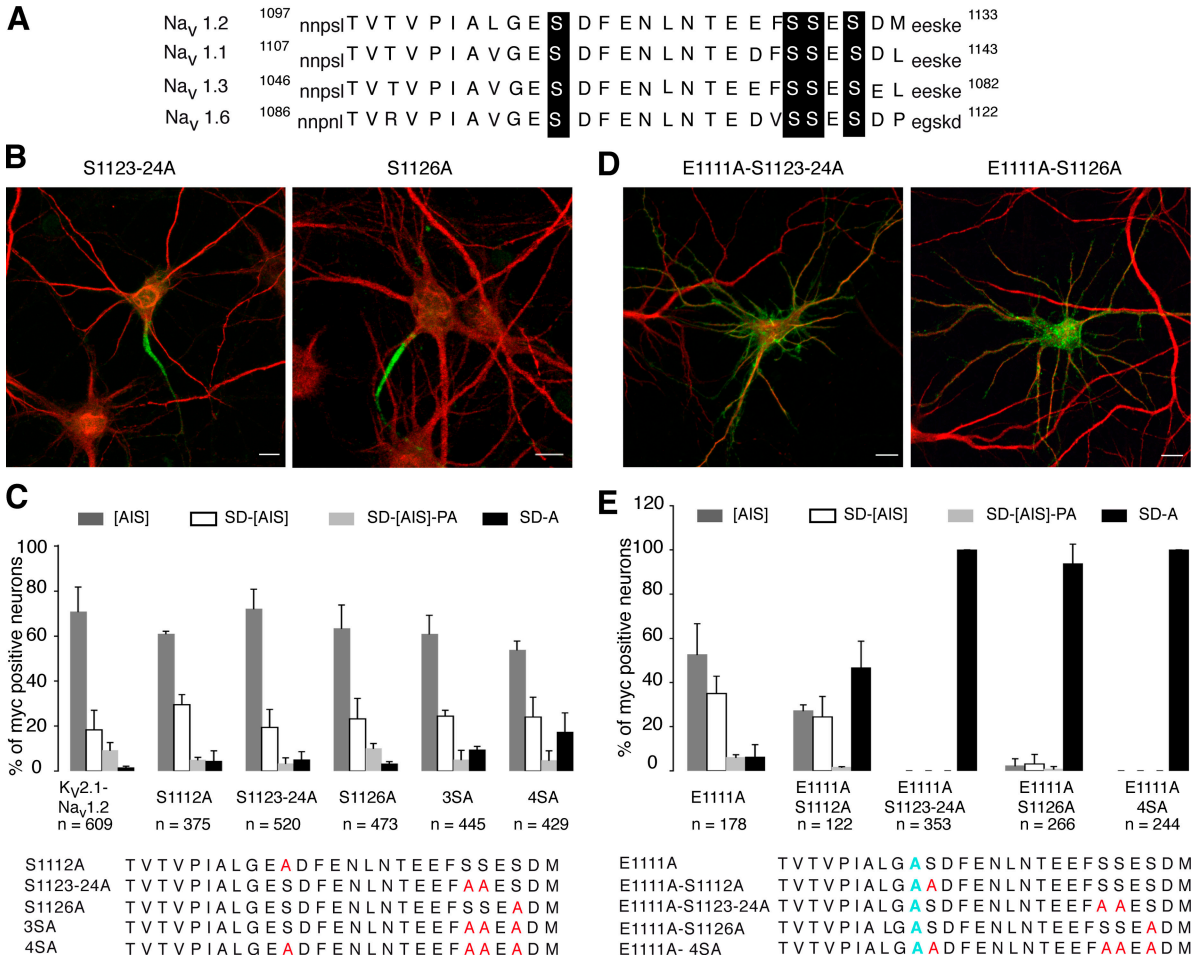

Figure 2. **Requirement for glutamate 1111 and serine residues for K$_V$2.1-Na$_V$1.2 compartmentalization at the AIS of hippocampal neurons.** (A) Schematic representation of the ankyrin-binding motif of sodium channels predominantly expressed in the CNS. Note the presence of four conserved serines (black boxes) and three potential serine phosphorylation sites for CK2 (Na$_V$1.2 S1112, S1124, and S1126). Numbers refer to the position of the amino acid residues in the corresponding Na$_V$1 types. (B–E) Cell surface distribution of K$_V$2.1-Na$_V$1.2 mutants. Cultured hippocampal neurons were transfected with the indicated constructs. 1 d after transfection, K$_V$2.1-Na$_V$1.2 was detected with an antibody to myc (green) before permeabilization, and the somatodendritic domain was subsequently identified by MAP2 staining (red). Mutations of different serine residues in the ankyrin-binding motif did not perturb K$_V$2.1-Na$_V$1.2 segregation at the AIS (B and C). In contrast, co-mutation of E1111 with serine residues induced a loss of K$_V$2.1-Na$_V$1.2 compartmentalization (D and E). (C and E) Histograms of the cell surface distribution of K$_V$2.1-Na$_V$1.2 mutants. The percentage of myc-positive neurons were classified into four categories: myc staining segregated at the AIS ([AIS]); distributed at the cell surface of the soma and proximal dendrites with an enrichment at the AIS (SD-[AIS]); enriched at the AIS with a distribution in soma, proximal dendrites, and axons (SD-[AIS]-PA); and uniformly distributed at the cell surface (non polarized; SD-A). 100% represents the total population of transfected neurons. Data are means ± SD from two to three different experiments; *n* denotes the total number of cells analyzed for each construct. Bars, 10 µm.

whether CK2 phosphorylation regulates the association of the ankyrin-binding motif and MBD-ankyrin (MBD-ank). With this aim, we used SPR technology (Wilson, 2002; Rich and Myszka, 2007). Purified GST-Na$_V$1.2 1,080–1,203 was immobilized on the sensor surface by immunoaffinity. GST–MBD-ank were purified, and the GST-tag was removed using PreScission Protease (see Materials and methods). When an increasing concentration of MBD-ankB was injected over flow cells, a weak surface reactivity was observed (Fig. 3 D). Binding analysis (see Materials and methods) indicated that these two domains associate with an apparent affinity constant (K_D) of 1.2 ± 0.4 10^{-6} M (Table I). When MBD-ankG was substituted for MBD-ankB, a similar affinity constant was obtained (a K_D of 1.7± 0.5 10^{-6} M; Table I). To evaluate the impact of phosphorylation on the interaction, CK2 phosphorylation was performed on immobilized GST-Na$_V$1.2 1080–1203, before either MBD-ankG or MBD-ankB injections (see Materials and methods). Under these conditions, increasing concentrations of MBD-ank injections produced a strongly increased binding signal. Kinetic analysis (see Materials and methods) of the interaction between MBD-ankG and the CK2-phosphorylated GST-Na$_V$1.2 1,080–1,203 gave an association rate (k_{on}) of 42.4 ± 41.6 10^5 $M^{-1}s^{-1}$ and a dissociation rate (k_{off}) of 2.1 ± 0.8 $10^{-3}s^{-1}$, resulting in a K_D of 0.9 ± 0.7 10^{-9} M. Similar binding affinities were obtained with MBD-ankB (Fig. 3 D and Table I). When GST-Na$_V$1.2 989–1,133 was immobilized on the sensor surface, interaction with MBD-ankB was also strongly modulated by CK2 phosphorylation (Fig. 3 E and Table I). These affinity constants were similar to those obtained with GST-Na$_V$1.2 1,080–1,203 (Table I), which indicates that they are independent of the type of immobilized GST-Na$_V$1.2 II-III constructs. We further examined the impact of Na$_V$1.2 E1111 on the association between

Published December 8, 2008

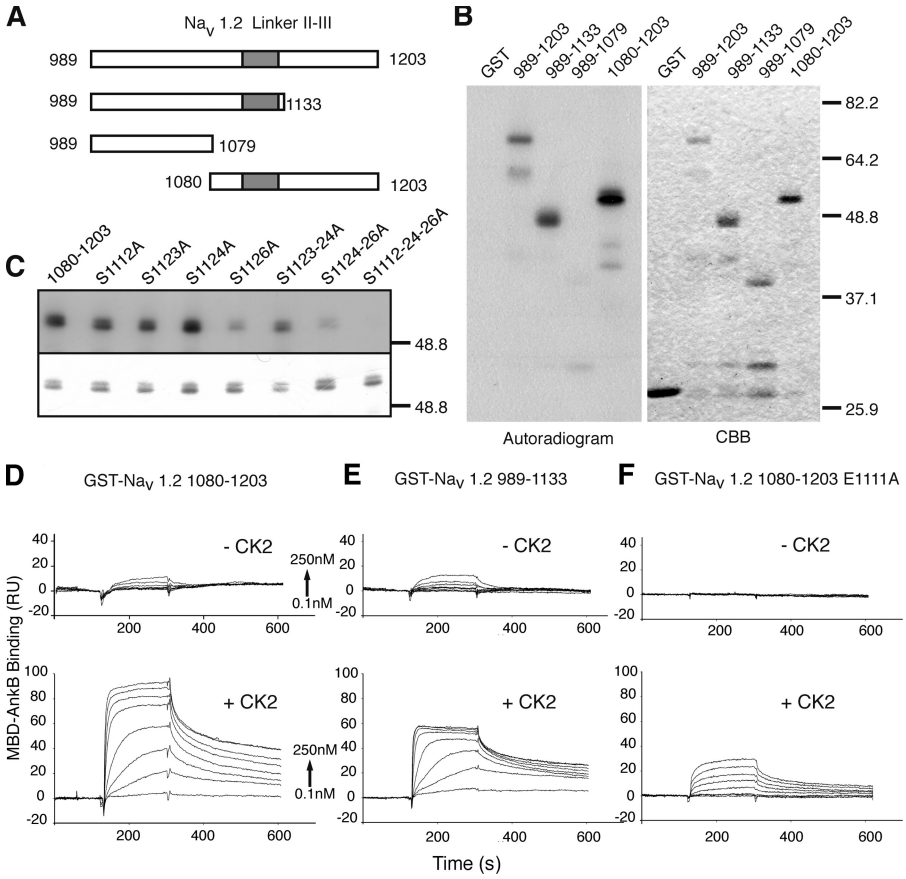

Figure 3. **CK2 phosphorylates the Na$_v$1.2 ankyrin-binding motif and regulates its interaction with MBD-ank.** (A–C) The Na$_v$1.2 ankyrin-binding motif is phosphorylated by CK2 in vitro. (A) Schematic representation of GST-Na$_v$1.2 linker II-III constructs. The position of the ankyrin-binding motif is indicated by gray boxes. Numbers refer to the position of corresponding amino acid residue in Na$_v$1.2. (B) The constructs were subjected to in vitro CK2 phosphorylation followed by SDS-PAGE. Coomassie brilliant blue staining (CBB) and ^{32}P incorporation revealed by autoradiography are shown. (C) The effect of site-directed serine mutations on CK2 phosphorylation of GST-Na$_v$1.2 II-III. CBB staining (bottom) and ^{32}P incorporation revealed by autoradiography (top) are shown. Numbers to the right of the gel blots indicate the molecular mass of standard markers (in kD). (D–F) SPR analysis of the interaction between the Na$_v$1.2 ankyrin-binding motif and MBD-ank. Typical sensorgrams are illustrated. Increasing concentrations of MBD-ankB ranging from 0.1 to 250 nM were injected over immobilized GST-Na$_v$1.2 1,080–1,203 (D), GST-Na$_v$1.2 989–1,133 (E), and GST-Na$_v$1.2 1,080–1,203 E1111A (F) before (top) and after in situ CK2 phosphorylation (bottom) of the immobilized constructs.

sodium channels and ankyrins by SPR. In the absence of phosphorylation, immobilized GST-Na$_v$1.2 1,080–1,203 E1111A failed to recruit MBD-ank (Fig. 3 F). After on-chip CK2 phosphorylation, GST Na$_v$1.2 1,080–1,203 E1111A associated with MBD-ank with an affinity constant (K_D) of 2.4 ± 0.8 10^{-8} M (Fig. 3 F and Table I). Finally, we evaluated the contribution of each of the serine residues of the ankyrin-binding motif on the phospho-dependent association between GST-Na$_v$1.2 1,080–1,203 and MBD-ank. The single serines to alanine mutation and double mutation S1123-24A did not modify the phospho-dependent association (Table II). The double mutation (S1124-26A) led to a decrease in affinity (K_D = 1.6 ± 1.3 10^{-7} M; Table II). The triple mutation robustly altered association, resulting in a 1,000-fold decrease in affinity (K_D = 2.6 ± 1.1 10^{-6} M; Table II). All together, these in vitro observations revealed that the association between the ankyrin-binding motif of neuronal sodium channels and the MBD of axonal ankyrins (MBD-ankG and MBD-ankB) is regulated by CK2 phosphorylation. These findings strongly suggest that CK2 is able to strengthen the interaction between ankyrin and sodium channels.

CK2 is highly enriched at the initial segment and in the nodes of Ranvier

If CK2 has a role in ankyrin–Na$_v$ interaction, one would expect that it is present at the AIS in vivo. To test this possibility, we looked at the subcellular localization of CK2 in neurons using a polyclonal antibody directed against the catalytic α subunit. In cultured hippocampal neurons, CK2 immunostaining was

Table I. **The effect of phosphorylation on the interaction between MBD-ank and the ankyrin-binding motif of sodium channels**

Immobilized construct	MBD	CK2 phosphorylation	k_{on}	k_{off}	K_D
			$M^{-1}s^{-1}$	s^{-1}	M
GST-Na$_v$1.2 1,080–1,203	ankG	–	NA	NA	1.7 ± 0.5 × 10^{-6a}
	ankB	–	NA	NA	1.2 ± 0.4 × 10^{-6a}
	ankG	+	42.4 ± 41.6 × 10^5	2.1 ± 0.8 × 10^{-3}	0.9 ± 0.7 × 10^{-9}
	ankB	+	28.0 ± 11.0 × 10^5	3.0 ± 0.1 × 10^{-3}	1.2 ± 0.4 × 10^{-9}
GST-Na$_v$1.2 989–1,133	ankB	–	NA	NA	1.3 ± 0.2 × 10^{-6a}
		+	60.1 ± 39.8 × 10^5	2.3 ± 0.1 × 10^{-3}	0.5 ± 0.2 × 10^{-9}
GST-Na$_v$1.2 1,080–1,203 E1111A	ankB	–	ND	ND	ND
		+	1.4 ± 0.3 × 10^5	3.2 ± 0.6 × 10^{-3}	2.4 ± 0.8 × 10^{-8}

Mean values ± SD were obtained from three to six experiments. ankB and ankG, ankyrin B and G, respectively; NA, not applicable; ND, no binding detected.
[a]K_D values were calculated using steady-state analysis (see Materials and methods).

Published December 8, 2008

Table II. **The effect of serine point mutations on the interaction between MBD-ank and the ankyrin-binding motif of sodium channels**

GST-Na_v 1.2 1,080–1,203 mutants	k_{on}	k_{off}	K_D
	$M^{-1}s^{-1}$	s^{-1}	M
S1112A	$8.9 \pm 0.2 \times 10^5$	$3.3 \pm 0.4 \times 10^{-3}$	$3.7 \pm 0.3 \times 10^{-9}$
S1123A	19.1×10^5	3.4×10^{-3}	1.8×10^{-9}[a]
S1124A	$16.3 \pm 3.2 \times 10^5$	$3.9 \pm 0.3 \times 10^{-3}$	$2.5 \pm 0.7 \times 10^{-9}$
S1126A	$16.2 \pm 14.4 \times 10^5$	$3.1 \pm 0.8 \times 10^{-3}$	$2.6 \pm 1.3 \times 10^{-9}$
S1123-24A	$8.2 \pm 2.6 \times 10^5$	$3.4 \pm 0.2 \times 10^{-3}$	$4.5 \pm 1.3 \times 10^{-9}$
S1124-26A	$0.9 \pm 1 \times 10^5$	$4.2 \pm 1.6 \times 10^{-3}$	$1.6 \pm 1.3 \times 10^{-7}$
S1112-24-26A	NA	NA	$2.6 \pm 1.1 \times 10^{-6}$[b]

Mean values ± SD are obtained from three to five experiments. NA, not applicable.

[a]Value from one experiment.

[b]K_D values were calculated using steady-state analysis (see Materials and methods).

concentrated in the AIS but not in the distal part of the axon (Fig. 4, A1–A3). CK2 was also visualized in nuclei (Filhol et al., 2003; Theis-Febvre et al., 2005), in soma, and in proximal dendrites. When hippocampal neurons were subjected to detergent extraction before cell fixation, CK2 immunostaining at the AIS was still observed (unpublished data), which suggests tethering to the cytoskeleton (Garrido et al., 2003; Fache et al., 2004). In vivo immunoreactivity for CK2 was further examined in the hippocampus (Fig. 4, B and C), cerebellum (Fig. 4 D), and cortex (Fig. S1, available at http://www.jcb.org/cgi/content/full/jcb.200805169/DC1). Initial segments were intensely immunoreactive for CK2 in all observed structures, as revealed by colabeling with ankyrin G (Figs. 4 and S1) and sodium channels (not depicted). Initial segments emanating from cell bodies of principal cells were observed in CA1 (Fig. 4, B and C), CA3, and dentate gyrus (Fig. S1, A and B). Initial segments positive for CK2 were also found in strati radiatum and oriens of CA1 and CA3, the molecular layer in the dentate gyrus, and in the hilus. Intense CK2 labeling appeared to underline the internal face of the plasma membrane of the initial segment, whereas the axoplasm displayed weak immunoreactivity, similar to ankyrin G localization (Fig. 4 B). In the hippocampus, 80% of ankyrin G–positive structures displayed a positive labeling for CK2 in the white matter ($n = 637$) and 88% in the gray matter ($n = 784$). CK2 was also detected in nuclei of neurons and putative glial cells (Fig. 4). Punctate labeling for CK2, colocalizing with ankyrin G, was observed in the alveus and white matter of forebrain and cerebellum (Fig. 5, A and B). In the cerebellum, 77% of ankyrin G–positive structures displayed a costaining with CK2 in the white matter ($n = 64$) and 88% in the gray matter ($n = 92$). Finally, CK2 immunoreactivity was present in the nodes of Ranvier of sciatic nerves (Fig. 5, C and D): 100% of the nodes of Ranvier were costained for ankyrin G and CK2 ($n = 40$). Collectively, these observations demonstrated that CK2 is a novel component of the AIS and of the nodes of Ranvier.

Evaluation of the role of the serine residues in the clustering of endogenous sodium channels

In addition to sodium channels, KCNQ2/KCNQ3 potassium channels are highly concentrated at the AIS both in cultured hippocampal neurons and in vivo, via an interaction with the MBD of ankyrin G (Devaux et al., 2004; Chung et al., 2006; Pan et al., 2006). We next addressed the question as to whether $K_v2.1$-$Na_v1.2$ acts as a dominant negative of sodium channel and KCNQ2/KCNQ3 potassium channel accumulation at the AIS. We therefore quantified immunostaining of endogenous sodium channels, KCNQ2/KCNQ3 channels, and ankyrin G in cells expressing $K_v2.1$-$Na_v1.2$ (transfected cells) and in nontransfected cells. The intensity of sodium channel staining was robustly reduced in $K_v2.1$-$Na_v1.2$–positive cells as compared with that observed in nontransfected cells, whereas ankyrin G staining was unmodified (Fig. 6, A and B). In contrast, KCNQ2/KCNQ3 staining intensity detected with an antibody directed against KCNQ3 was equivalent in cells expressing $K_v2.1$-$Na_v1.2$ and in nontransfected cells (Fig. 6, A and C). This strongly suggested that the presence of $K_v2.1$-$Na_v1.2$ specifically disturbed the accumulation of sodium channels but not KCNQ2/KCNQ3.

Our SPR analysis demonstrated that the association between sodium channels and the MBD of axonal ankyrins is regulated by CK2 phosphorylation. Immunostaining, both in cultured neurons and in vivo, revealed that CK2 is highly enriched at the AIS and in the nodes of Ranvier. These observations led us to examine the possibility that CK2-mediated phosphorylation of sodium channels occurs locally, at the AIS, contributing to channel clustering. We thus examined whether the perturbation of endogenous sodium channel accumulation induced by $K_v2.1$-$Na_v1.2$ was dependent on CK2 phosphorylation sites. Upon mutation of a single serine into alanine (S1112A and S1126A, respectively), mutated $K_v2.1$-$Na_v1.2$ induced a decrease in sodium channel staining intensity, like $K_v2.1$-$Na_v1.2$ (unpublished data). When the three serine residues located in the C-terminal end of the AIS motif were all mutated into alanines, the effect of the corresponding mutant (3SA) was less pronounced than with $K_v2.1$-$Na_v1.2$ (Fig. 6 B). The abrogation of four serine residues into alanines (4SA) impaired the dominant-negative effect of $K_v2.1$-$Na_v1.2$ on sodium channel clustering (Fig. 6, A and B). These findings revealed that expression of phosphorylation-deficient AIS motif constructs failed to perturb sodium channel accumulation in cultured neurons.

The effect of a CK2 inhibitor on the accumulation of sodium channels at the AIS of cultured hippocampal neurons

To further demonstrate that CK2 is involved in the accumulation of sodium channels at the AIS, we evaluated the effect of

Published December 8, 2008

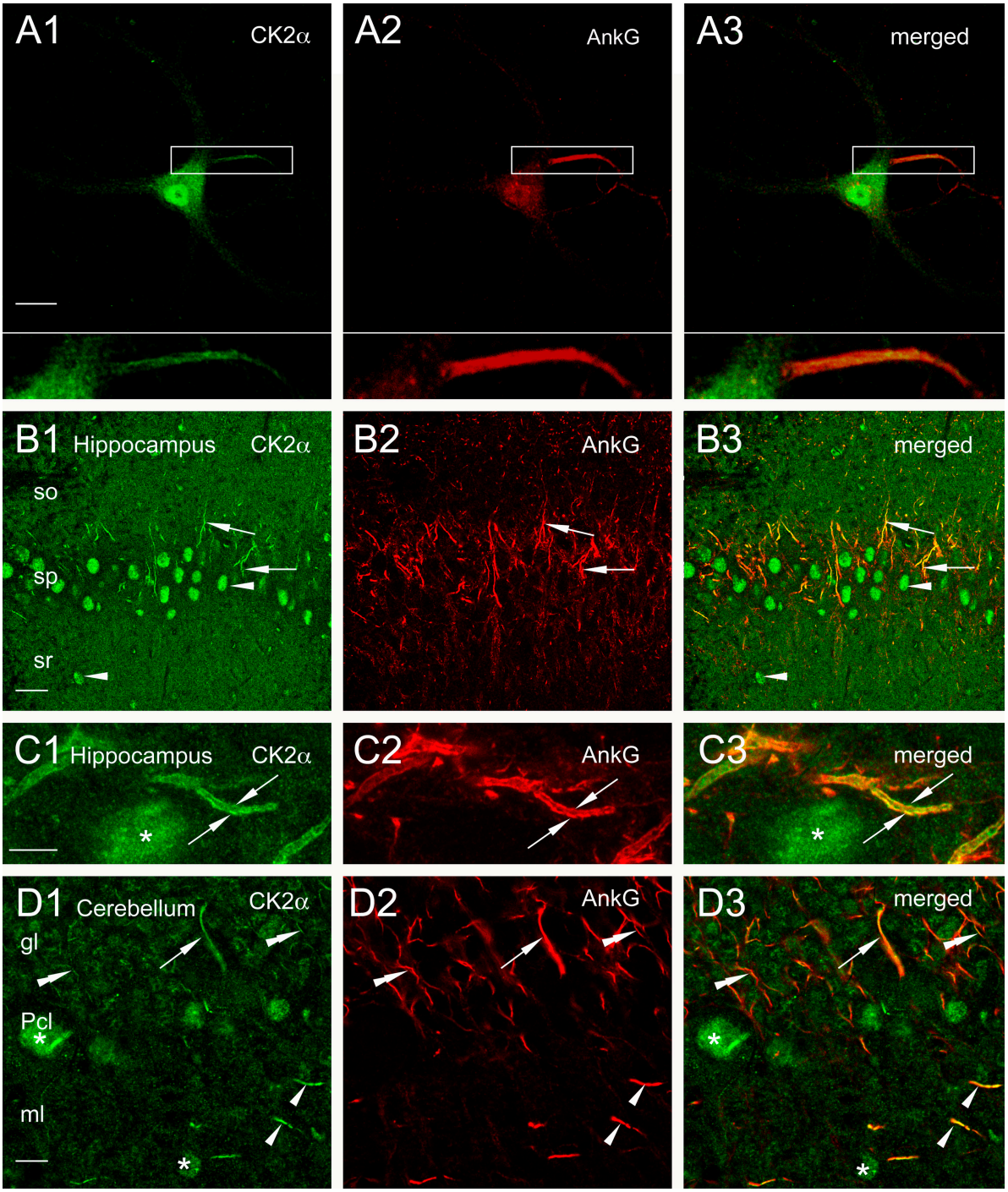

Figure 4. **CK2α is concentrated at AISs.** (A) A cultured hippocampal neuron was immunostained for CK2α (A1) and ankyrin G (A2). CK2α immunoreactivity is highly expressed in the initial segment (box). Enlarged views of the initial segment are visualized in A1–A3, bottom. (B and C) In the CA1 area of the hippocampus, CK2α immunoreactivity is visible within nuclei (B1, arrowheads) of putative pyramidal cells and interneurons. As demonstrated by colabeling with ankyrin G (B2, arrows), CK2α is present in initial segments all over the different strati (B1 and B3, arrows). CK2α shows light and diffuse additional staining within the neuropil. CK2α immunoreactivity (C1 and C3, arrows) and ankyrin G labeling (C2, arrows) are concentrated along the cytoplasmic membrane of an initial segment in the stratum pyramidale next to a CK2α-labeled nucleus (C1 and C3, asterisks). (D) In cerebellum, nuclei (D1, asterisk) of Purkinje cells and interneurons of the molecular layer (ml) are labeled for CK2. Coimmunolabeling for CK2α (D1) and for ankyrin G (D2) is visible within initial segments of a putative Purkinje cell (D1–D3, arrows), granular cells (D1–D3, double arrowheads), and interneurons (D1–D3, single arrowheads). gl, granular layer; Pcl, Purkinje cell layer, so, stratum; sp, stratum pyramidale; sr, stratum radiatum. Bars: (A) 23 µm; (B) 26.8 µm; (C and D) 6.82 µm.

2-dimethylamino-4,5,6,7-tetrabromo1*H*-benzimidazole (DMAT), a CK2 inhibitor (Pagano et al., 2004), in cultured hippocampal neurons (Fig. 7). The immunostaining of ankyrin G and $Na_v.1$ channels was quantified in neurons treated with either DMAT or DMSO (control cells) at two stages of maturation. It has been shown previously that the percentage of cells with an AIS increases between 2 and 4 d in vitro (DIV; Yang et al., 2007; Martin et al., 2008). The inhibition of CK2 activity in immature

Published December 8, 2008

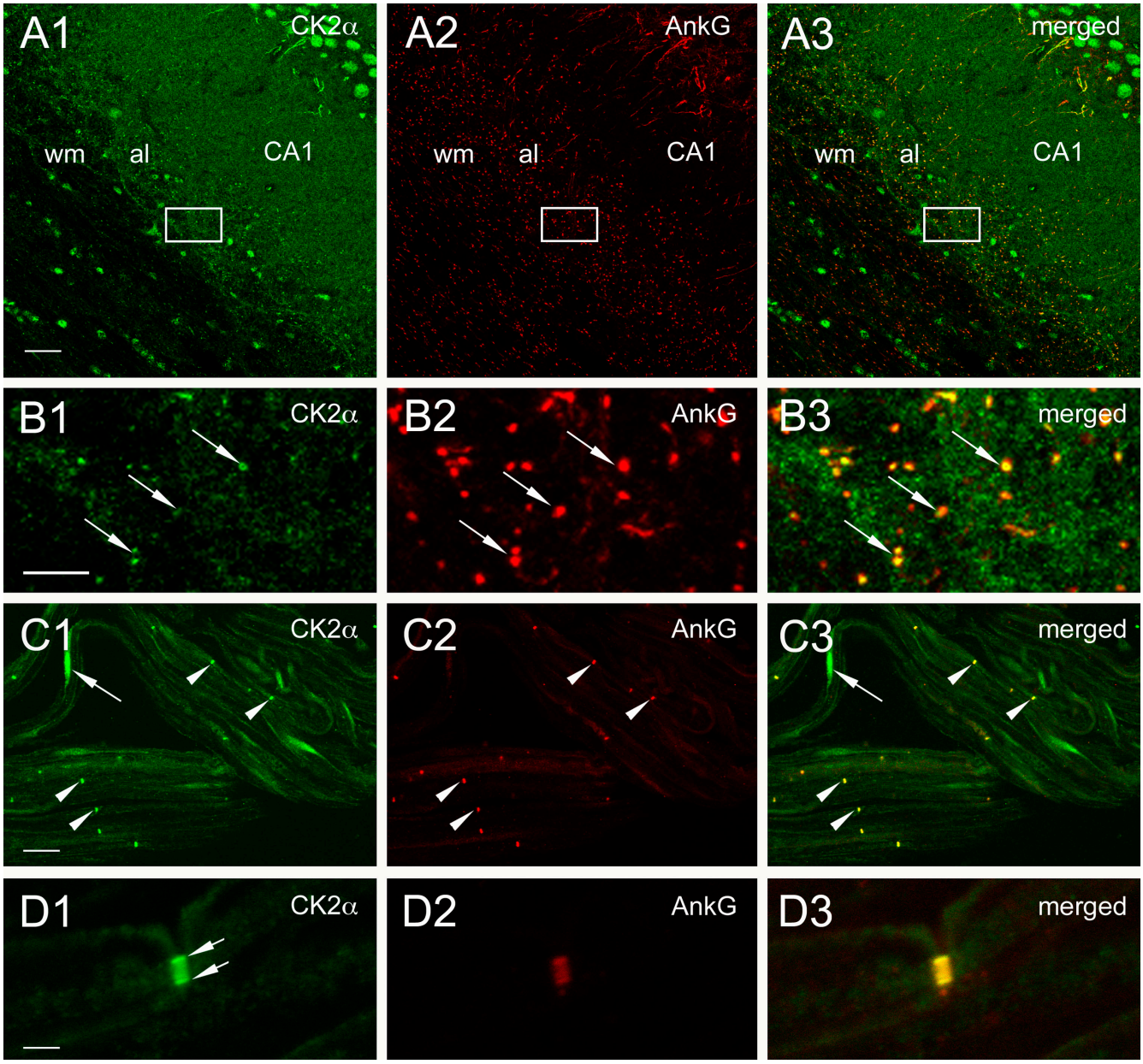

Figure 5. **CK2α is concentrated in CNS and PNS nodes of Ranvier.** (A and B) CK2α immunoreactivity is visible as numerous punctiform structures (B1 and B3, arrows) colabeled for ankyrin G (B2 and B3, arrows) within the alveus and cortical white matter that probably correspond to nodes. B1–B3 are enlarged views of the boxed areas in A1–A3. (C and D) Ranvier nodes are labeled for CK2α and ankyrin G (C1–C3, arrowheads) in teased fibers of the sciatic nerve. CK2α labeling is concentrated at the membrane of the nodal region (D1, arrows). CK2α immunoreactivity is also visible in the nucleus of a Schwann cell (e.g., C1 and C3, arrows). al, alveus; wm, white matter. Bars: (A) 26.8 µm; (B) 6. 71 µm; (C) 23.2 µm; (D) 3 µm.

cells (from 2 to 4 DIV) induced an increase in the number of cells negative for ankyrin G staining as compared with what was observed in control cells. In the other cell population (ankyrin G–positive), we observed a decrease in the staining intensity of ankyrin G and $Na_v.1$ channels (Fig. 7, A and B). At 9 DIV, all the cells present an AIS (Yang et al., 2007; Martin et al., 2008). The addition of DMAT in the culture medium of neurons at 9 DIV during 30 h induced a decrease in ankyrin G and $Na_v.1$ channels staining (Fig. 7, C and D). These results showed that inhibition of CK2 activity perturbs the accumulation of sodium channels and ankyrin G at two different stages of AIS organization.

Discussion

CK2 phosphorylation regulates the interaction between neuronal sodium channels and ankyrin

We previously identified a determinant of 27 residues (Garrido et al., 2003), called the AIS motif, that includes the PIALGESD sequence defined by Lemaillet et al. (2003). In close agreement with our previous work (Garrido et al., 2003), we show here that the determinant required for high-affinity ankyrin binding is not restricted to the PIALGESD sequence but extends further toward the C-terminal sequence, including two CK2 phosphorylation

Published December 8, 2008

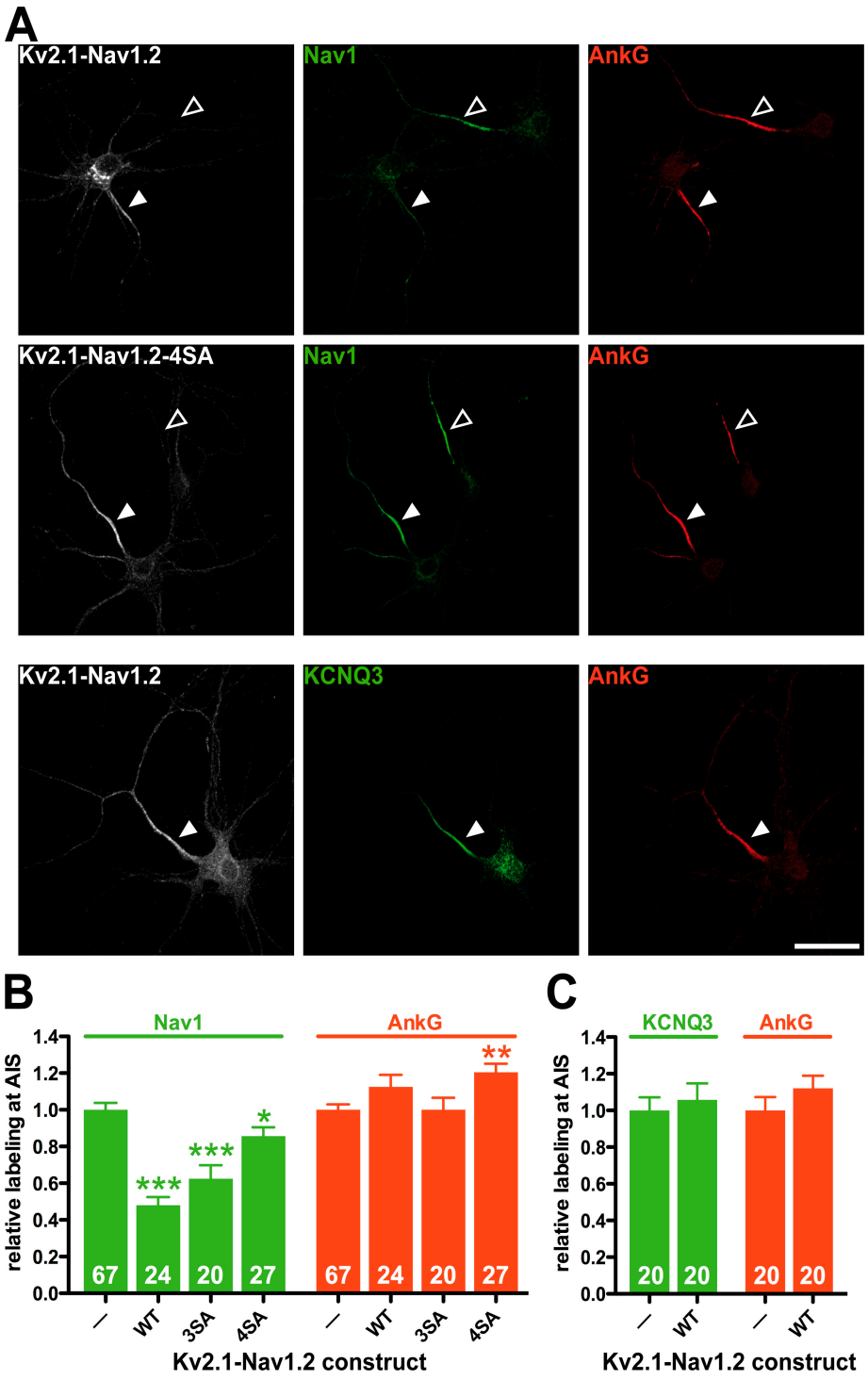

Figure 6. **Impact of $K_v2.1$-$Na_v1.2$ and of phosphorylation-deficient $K_v2.1$-$Na_v1.2$ constructs on the accumulation of sodium channels (Na_v1) and KCNQ2/KCNQ3 potassium channels at the AIS of cultured hippocampal neurons.** (A, top and middle) $K_v2.1$-$Na_v1.2$ expression perturbed Na_v1 accumulation at the AIS, unlike the phosphorylation-deficient $K_v2.1$-$Na_v1.2$ 4SA mutant. Hippocampal neurons were transfected with either $K_v2.1$-$Na_v1.2$ or phosphorylation-deficient $K_v2.1$-$Na_v1.2$ mutants. Then cells were stained for myc (gray), ankyrin G (red), and sodium channels (green). (B) Quantification of Na_v1 and ankyrin G staining intensity in untransfected cells (A, open arrowheads) and in transfected cells (closed arrowheads). (A, bottom) $K_v2.1$-$Na_v1.2$ expression did not perturb KCNQ3 accumulation at the AIS. Cells transfected with $K_v2.1$-$Na_v1.2$ were subsequently stained for myc (gray), ankyrin G (red), and KCNQ3 potassium channels (green). (C) Quantification of KCNQ3 and ankyrin G staining intensity. Fluorescence intensity measured in transfected cells, identified by myc staining, was normalized by taking as 100% the staining intensity measured in nontransfected cells (arrowheads). Numbers at the base of the bars denote the number of quantified cells. Error bars indicate mean ± SEM. Mann-Whitney test: *, $P < 0.05$; **, $P < 0.01$; ***, $P < 0.001$. WT, wild type. Bars, 10 µm.

Published December 8, 2008

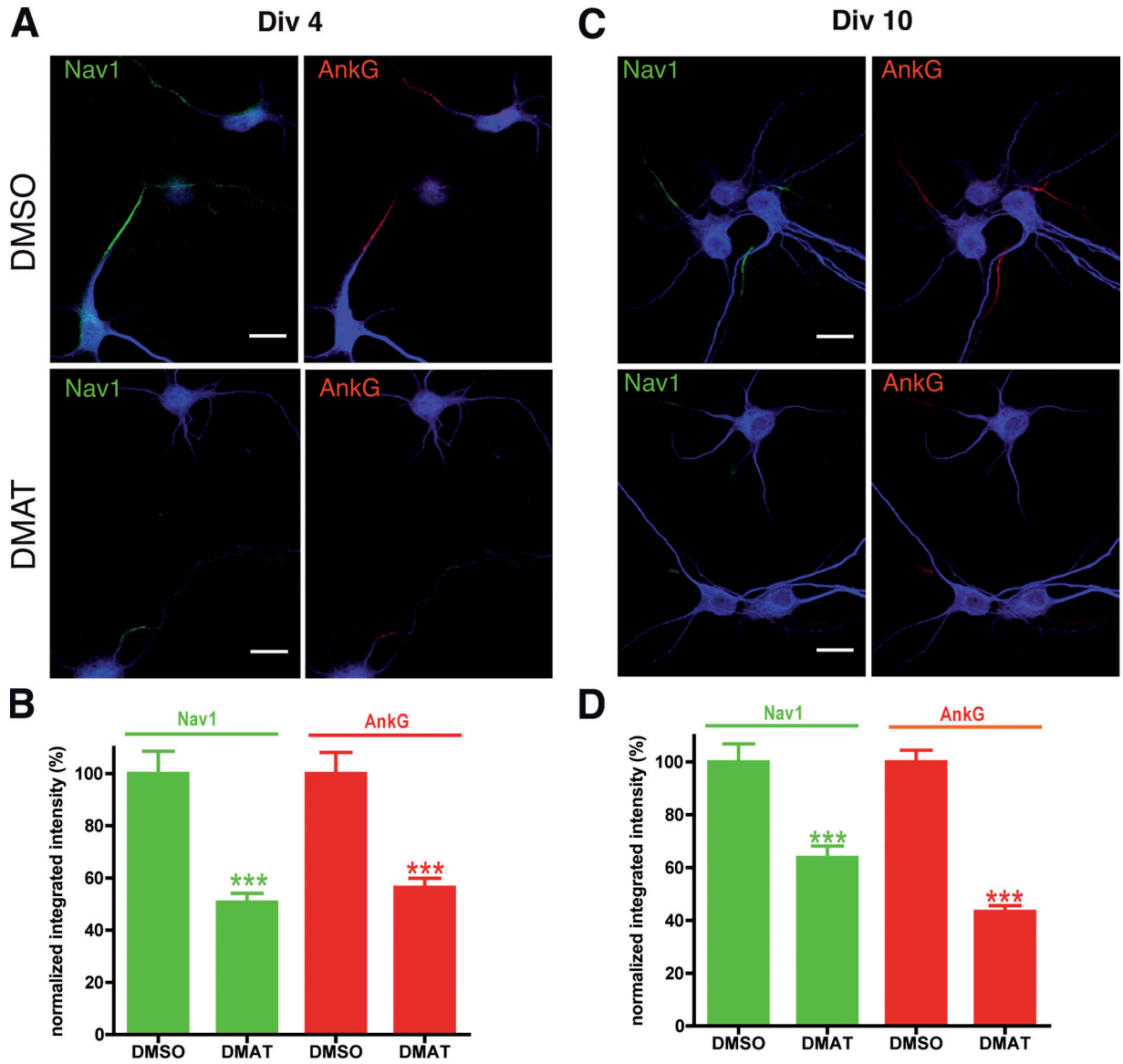

Figure 7. **The effect of a CK2 inhibitor on the accumulation of sodium channels at the AIS of cultured hippocampal neurons.** Cultured hippocampal neurons were treated with either DMAT (50 μM) or with DMSO (control cells) either from 2 to 4 DIV (A and B) or from 9 to 10 DIV (C and D). They were subsequently immunostained for Na_v1 channels (green), ankyrin G (red), and MAP2 (blue). (B and D) Quantification of Na_v1 and ankyrin G staining intensity. Fluorescence intensity was normalized by taking as 100% the staining intensity measured in control cells. The results are from three independent experiments, the number of quantified AIS ranged from 70 to 230. Error bars indicate mean ± SEM. *t* test: ***, $P < 0.0001$. Bars, 10 μm.

sites ($Na_v1.2$ S1124 and S1126). In addition, we provide here the first evidence that the interaction between the ankyrin-binding motif and the MBD of ankyrins is regulated by CK2. This conclusion is based on the following findings. First, we observed that the AIS motif of CNS sodium channels is phosphorylated in vitro by CK2. This was supported by the abrogation of S1124-26 located in the C-terminal region of the AIS motif, which inhibited phosphorylation. Second, a quantitative binding assay based on SPR revealed that CK2 phosphorylation of the AIS motif resulted in a 1,000-fold increase (from $1.2\ 10^{-6}$ M to $1.2\ 10^{-9}$ M) of the binding affinity for MBD-ank. This effect was observed using two distinct constructs in which the ankyrin-binding motif was localized distally or proximally with respect to GST. Besides, CK2 phosphorylation was equally effective for interactions with the MBD of ankyrin B and G. In addition, it was profoundly altered upon mutation of two to three serine residues. Co-mutation of S1124 with S1126 induced a robust decrease in binding affinity from $1.2\ 10^{-9}$ M to $1.6\ 10^{-7}$ M. Third, we observed that $K_v2.1$-$Na_v1.2$ segregation at the AIS required the cooperation of two motifs: $Na_v1.2$ E1111 and the serine residues S1112, S1124, and S1126. Co-mutation of E1111 with either S1124 or S1126 was found to be more effective than E1111-S1112 mutations. Fourth, we observed that expression of phosphorylation-deficient AIS motif constructs failed to perturb sodium channel accumulation in cultured neurons (Fig. 6). At the steady-state surface distribution, all the $K_v2.1$-$Na_v1.2$ serine mutants were predominantly compartmentalized at the AIS (Fig. 2, B and C), which indicates that the loss of the dominant-negative effect of $K_v2.1$-$Na_v1.2$ induced by serine mutations did not result from deficient AIS localization but

Published December 8, 2008

rather from the conversion of serines into alanines. Finally, we observed that inhibition of CK2 activity perturbed sodium channel accumulation at two distinct stages of AIS formation. Considered together, our findings show that several CK2 phosphorylation sites regulate the interaction between CNS sodium channels and ankyrins.

What is the contribution of the glutamate residue ($Na_v1.2$ E1111)? SPR analysis revealed that the $Na_v1.2$ E1111A mutation totally abolished basal MBD-ank binding in the micromolar range measured in the absence of CK2 phosphorylation (Fig. 4). After CK2 phosphorylation, the binding affinity of the $Na_v1.2$ E1111A mutant was affected ($K_D = 2.4\ 10^{-8}$ M) when compared with the control ($K_D = 1.2\ 10^{-9}$ M), but it remained high. This strongly suggests that different CK2 phosphorylation sites of the ankyrin-binding motif can overcome the E1111A mutation. However, we cannot totally exclude the possibility that our experimental conditions favored a high degree of phosphorylation of the ankyrin-binding motif. This may highlight the structural requirement for multiple serine phosphorylation and underestimate the contribution of residue E1111. $Na_v1.2$ E1111 mutation was found to alter the level of cell surface expression of $K_v2.1$-$Na_v1.2$ in cultured hippocampal neurons (Fig. 1), which is in close agreement with a previous study on $Na_v1.5$ (Mohler et al., 2004). However, this mutation did not impair $K_v2.1$-$Na_v1.2$ segregation at the AIS because of the contribution of the phosphoserine residues. The fact that the association of E1111A with either S1124 or S1126 mutations was mandatory for the loss of $K_v2.1$-$Na_v1.2$ segregation at the AIS was consistent with this conclusion. Our findings strongly suggest that phosphorylation of three serine residues of the ankyrin-binding motif tunes the trafficking of sodium channels and their accumulation at discrete sites in neurons. It is noteworthy that variable phosphorylation of sites on the $K_v2.1$ potassium channel allows graded activity-dependent regulation of channel gating and neuronal firing properties (Misonou et al., 2006; Park et al., 2006). Hence, multiple phosphorylation is likely to constitute an important regulatory mechanism for both the activity and the trafficking of voltage-gated ion channels in neurons.

CK2 is a novel component of the AIS and of the nodes of Ranvier

CK2 is constitutively active and involved in a large spectrum of biological processes, including cell proliferation, apoptosis, and the circadian clock (Meggio and Pinna, 2003). Our data provide the first evidence that CK2 is a component of the AIS and the node of Ranvier in neurons. CK2 is a tetramer composed of two catalytic α subunits and two β subunits (Filhol et al., 2004). Immunostaining of the catalytic α subunit of CK2 at the AIS was observed in all the CNS regions examined (hippocampus, cortex, and cerebellum). It was also found in CNS and PNS nodes of Ranvier. The question remains open as to whether the CK2β subunit is also concentrated within these two subdomains. CK2 localization revealed submembrane recruitment with ankyrin G within the AIS, which presumably regulates not only interaction between sodium channels and ankyrin G but also the complex interplay with other axonal components. Consistently, we observed that inhibition of CK2 activity perturbed ankyrin G concentration during the formation and the maintenance of the AIS. It is possible that CK2 regulates ankyrin G binding to β IV spectrin, as described in chicken erythrocytes (Ghosh et al., 2002). Furthermore, the involvement of the potential CK2 phosphorylation sites located in the C terminus of potassium channels KCNQ2 and KCNQ3 in accumulation at the AIS and in the nodes of Ranvier deserves close examination (Chung et al., 2006; Pan et al., 2006). Crosstalk between nuclear factor κB (Politi et al., 2007; Schultz et al., 2006) and CK2 signaling pathways might occur. Hence, an important issue in the future will be to obtain more information on the regulatory role of CK2 in the specification and the maintenance of the AIS and the nodes of Ranvier.

The role of CK2 in positioning sodium channels in ankyrin G–positive domains

In neurons, biochemical and genetic studies have shown that sodium channel accumulation is an ankyrin-based mechanism occurring via a direct interaction with MBD, a domain highly conserved in ankyrin G and B (Lemaillet et al., 2003; Mohler et al., 2004). Our SPR assay revealed that the $Na_v1.2$ ankyrin-binding motif recognized MBD-ankG as well as MBD-ankB with an equivalent binding affinity (Table I). However, a high density of sodium channels occurs only in ankyrin G subdomains both in vivo and in cultured neurons (Boiko et al., 2001, 2003; Garrido et al., 2003; Fache et al., 2004; Dzhashiashvili et al., 2007). In addition, distinct chimeras bearing the ankyrin-binding motif of sodium channels, including $K_v2.1$-$Na_v1.2$ (Fig. 1), were found to be concentrated at AIS (positive for ankyrin G) but not distal axons (positive for ankyrin B) of cultured hippocampal neurons (Garrido et al., 2003; Lemaillet et al., 2003; Fache et al., 2004; Pan et al., 2006). How can we explain the discrepancy between in vivo localization of sodium channels and in vitro assays? The intramolecular interaction between the N and the C termini of ankyrin B could impede sodium channel recognition of the MBD (Abdi et al., 2006). In the view of our findings, it is tempting to propose that CK2 regulates sodium channel interaction with ankyrin G and thus contributes to their specific accumulation at the AIS and the nodes of Ranvier. The local concentration of CK2 at the AIS and in the nodes of Ranvier could lead to phosphorylation of Na_v sodium channels at their ankyrin-binding domain. It also possible that a ménage à trois between ankyrin G, Na_v channels, and CK2 is involved in the sorting of these components to the AIS and nodes of Ranvier. This phosphorylation-based process could represent a striking example of how posttranslational modifications can fine tune interactions between key protein partners. Neuronal cells are likely to rely on such a dynamic network of modulated interactions to attain an exquisite level of subcellular compartmentalization. Moreover, these regulated interactions likely contribute to the inherent plasticity of neurons, allowing them to dynamically adjust protein localization as a response to their various inputs. Precisely, the possibility of a dynamic modulation of ankyrin–Na_v interaction by synaptic activity is a fascinating question that should be addressed in future studies.

Published December 8, 2008

Materials and methods

DNA constructs

Rat $K_v2.1$ cDNA was a donation from O. Pongs (University of Hamburg, Hamburg, Germany). The extracellular myc epitope was inserted in the pCDNA3-$K_V2.1$ using a QuikChange XL mutagenesis kit (Agilent Technologies). The myc-$K_v2.1$-$Na_v1.2$ 1,080–1,203 ($K_v2.1$-$Na_v1.2$) chimera was constructed by P. Giraud (Institut National de la Santé et de la Recherche Médicale, Unité Mixte de Recherche 641, Marseille, France) by sequential PCR amplification using Expand High Fidelity Taq DNA polymerase (Roche).

Full-length $Na_v1.2$ linker II-III and truncated fragments were cloned into NcoI–NotI sites of the derived pGEX-6P vector (GE Healthcare). Site-directed mutants were obtained from pcDNA3-$K_v2.1$-$Na_v1.2$ or pGEX-6P-$Na_v1.2$ 1,080–1,203. pGEX-6P-MBD-ankB (amino acids 1–957 of human 220-kD ankyrin B) and rat 270-kD ankyrin G were provided by V. Bennett (Duke University Medical Center, Durham, NC). MBD-ankG constructs were generated by PCR (amino acids 1–981 of Rat 270-kD ankyrin G) and cloned into BamHI–Not I sites of the derived pGEX-6P vector. All the generated constructs were verified by DNA sequencing.

Recombinant protein expression and purification

GST-tagged protein were expressed in *Escherichia coli* strain BL21 or Rosetta2 (DE3) and purified by glutathione–Sepharose 4B according to the manufacturer's instructions (GE Healthcare). MBD-ankG or MBD-ankB proteins were cleaved from GST using PreScission Protease (GE Healthcare). Protein concentrations were determined using a Bradford assay.

In vitro phosphorylation assay

GST fusion proteins (1–5 µg) were suspended in 50 µl of kinase buffer (20 mM Tris-HCl, 50 mM KCl, and 10 mM $MgCl_2$, pH 7.5) containing 200 µM ATP (Invitrogen) and 10 µCi γ-ATP (GE Healthcare), then incubated with 10 units of CK2 (New England Biolabs, Inc.) for 20 min at 30°C. Samples were analyzed on 12% SDS-PAGE. Coomassie brilliant blue staining revealed bands, and labeled components were detected by autoradiography.

SPR experiments

SPR experiments were performed at 25°C on a Biacore 3000 instrument (GE Healthcare) with CM5 sensor chips, using 10 mM Hepes-NaOH, pH 7.4, 150 mM NaCl, 3 mM EDTA, and 0.005% surfactant P20 as the running buffer (GE Healthcare). Approximately 5–7 fmol of GST fusion proteins and GST were immobilized in flow cells via anti-GST polyclonal goat antibody covalently coupled using the amine-coupling chemistry. CK2 phosphorylation was directly performed onto chip according to Catimel et al. (2006), and 1 M NaCl was used to eliminate residual CK2. Purified MBD-ankB or MBD-ankG (0.1–7,000 nM) were injected at a flow rate of 20 µl/min for 3 min. After 5 min of dissociation, the chip was regenerated with 1 M NaCl for 3 min. All sensorgrams show data in which the non-specific signal (GST) was subtracted from the total signal (GST fusion protein). The K_D for MBD-ankB or MBD-ankG with CK2-untreated proteins or with a CK2-treated S1112-24-26A mutant was calculated by plotting saturation binding curves using the equilibrium response value at a plateau of all curves. The K_D and the rate constants for MBD-ankB or MBD-ankG (analyte concentrations between 0.1 to 10 K_D) with phosphorylated proteins were calculated by global fitting using a single-site interaction model. The χ^2 values were in the range of 0.1–20.

Cell culture, transfection, and inhibition of CK2 activity

Primary hippocampal neurons were prepared as described previously (Goslin and Banker, 1989; Garrido et al., 2003). Neurons were transfected after 9 DIV using Lipofectamine 2000 (Invitrogen) in the presence of 1 mM kynurenate (Sigma-Aldrich) and 10 mM $MgCl_2$. The conditioned medium was supplemented with 10 µM D(-)-2-amino-5-phosphonopentanoic acid (Tocris Bioscience). Transfected cells were processed for immunofluorescence 18 h after transfection. The inhibition of CK2 activity was performed using DMAT (EMD) as a CK2 inhibitor (Pagano et al., 2004). DMAT was dissolved in DMSO at 10 mM and was added to the culture medium of hippocampal neurons at a final concentration of 50 µM. 24 h later, 25% of DMAT was added to compensate for degradation loss of inhibitor activity. The same amounts of DMSO were added in sister cells (i.e., negative control).

Antibodies

Mouse monoclonal antibodies included antibodies to myc (1:100; Roche), MAP2 (1:400; Sigma-Aldrich), and sodium channel (pan Na_v; 1:100–400; Sigma-Aldrich). Rabbit polyclonal antibodies included MAP2 (1:500; Millipore), ankyrin G (1:500–1,000; a gift from G. Alcaraz, Institut National de la Santé et de la Recherche Médicale, Unité Mixte de Recherche 641, Marseille, France), and KCNQ3 (1:800; Alomone Labs). A goat polyclonal antibody to CK2α (1:50; Santa Cruz Biotechnology, Inc.) and a chicken polyclonal antibody to myc and MAP2 (1:250 and 1:10,000, respectively; Abcam) were used. Secondary goat and donkey antibodies conjugated to Alexa Fluor 488, 546, 568, and 633 (Invitrogen) or Cy5 (Jackson ImmunoResearch Laboratories) were used at 1:400–800 dilutions.

Immunofluorescence

To detect the steady-state surface distribution of the $K_v2.1$-$Na_v1.2$ chimera in transfected hippocampal neurons, nonspecific binding was blocked with 0.22% gelatin in 0.1 M phosphate buffer (PB) after PFA fixation. Cells were incubated for 1 h with antibody to myc. Endogenous proteins (ankyrin G, MAP2, CK2α, and sodium channel) were immunodetected after a permeabilization step (0.066% saponin and 0.22% gelatin in PB), preceded by a brief incubation with 20% of Triton X-100 for pan sodium channel antibodies. Corresponding secondary antibodies conjugated to Alexa Fluor or Cy5 were incubated for 1 h. Coverslips were mounted in Fluor Save reagent (EMD).

Immunohistochemistry

All procedures were in agreement with the European Communities Council directive (86/609/EEC). Cerebella and forebrain from Wistar adult rats were removed and immediately frozen in cold isopentane (−50°C). Brain sections were obtained on a cryostat and fixed by immersion in phosphate buffer containing 4% PFA for 15 min. Sciatic nerves were dissected and placed for 1 h in fixative. After teasing, fibers were transferred to slides and allowed to air dry. After 1 h incubation in 10% normal donkey serum in PBS, tissues were incubated overnight in primary antibodies (mouse antibody to pan Na_v, goat antibody to CK2α, and rabbit antibody to ankyrin G). After washes, secondary antibodies diluted in PBS 0.1 M, pH 7.4, containing 0.3% Triton X-100 were applied for 2 h.

Confocal microscopy and quantification

Immunofluorescence slides were imaged using a confocal microscope (TCS-SPE or TSC-SP2; LCS or LAS-AF software; Leica). Confocal images were acquired with 40×/1.25 NA, 63×/1.32 NA, or 63×/1.40 NA oil objectives (Leica) at ambient temperatures. Fluorescence was collected as z stacks with sequential wavelength acquisition. Quantification was performed using ImageJ software (http://rsb.info.nih.gov/ij/). Regions of interest corresponding to AIS were manually selected on ankyrin G and/or Na_v1 images and reported on other channels for intensity measurements. All intensities were corrected for background labeling. Image editing was performed using ImageJ or Photoshop 7.0 (Adobe) and was limited to rolling-ball background subtraction, linear contrast enhancement, and gamma adjustment.

Online supplemental material

Fig. S1 shows the colocalization of endogenous CK2α and ankyrin G in the hippocampus, dentate gyrus, and cortex. Online supplemental material is available at http://www.jcb.org/cgi/content/full/jcb.200805169/DC1.

We thank R. Miquelis and C. Lévêque for their advice for SPR experiments and data analysis; O. Pongs for providing $K_v2.1$ cDNA; V. Bennett for providing GST-MBD-ankB and ankyrin G-GFP cDNA; P. Giraud for constructing myc-$K_v2.1$-$Na_v1.2$; G. Alcaraz for providing the polyclonal antibody to ankyrin G; L. Fronzaroli-Molinieres, J.C. Graziano, and A. Malzac for preparation of cultured hippocampal neurons; Centre de Microscopie et d'Imagerie of Institut Fédératif de Recherche 11 for imagery facilities; O. Filhol-Cochet for helpful discussions; and F. Castets, H. Vacher, and M. Seagar for critical reading of the manuscript.

This work was supported by the Institut National de la Santé et de la Recherche Médicale, the Ministère de la Recherche, the Association Française contre les Myopathies (grant NM2-2006-12207), the Association pour la Recherche de la Sclérose en Plaque, the Agence Nationale pour la Recherche (grant ANR-05-NEUR-012), and the Fondation pour la Recherche Médicale (grant DEQ20051205734-FRM Equipe 2005). We thank the Centre National de la Recherche Scientifique for additional financial support to A. Baude, G. Ferracci, and B. Dargent. S. Pereira was a recipient of the Association pour la Recherche de la Sclérose en Plaque and the Association Française contre les Myopathies, C. Leterrier of the Agence Nationale pour la Recherche, and M. Irondelle of the Fondation pour la Recherche Médicale. A. Bréchet and A. Brachet were supported by a fellowship from the Ministère de la Recherche.

Submitted: 28 May 2008
Accepted: 7 November 2008

References

Abdi, K.M., P.J. Mohler, J.Q. Davis, and V. Bennett. 2006. Isoform specificity of ankyrin-B: a site in the divergent C-terminal domain is required for intramolecular association. *J. Biol. Chem.* 281:5741–5749.

Alessandri-Haber, N., C. Paillart, C. Arsac, M. Gola, F. Couraud, and M. Crest. 1999. Specific distribution of sodium channels in axons of rat embryo spinal motoneurones. *J. Physiol.* 518:203–214.

Basak, S., K. Raju, J. Babiarz, N. Kane-Goldsmith, D. Koticha, and M. Grumet. 2007. Differential expression and functions of neuronal and glial neurofascin isoforms and splice variants during PNS development. *Dev. Biol.* 311:408–422.

Bennett, V., and S. Lambert. 1999. Physiological roles of axonal ankyrins in survival of premyelinated axons and localization of voltage-gated sodium channels. *J. Neurocytol.* 28:303–318.

Blom, N., T. Sicheritz-Ponten, R. Gupta, S. Gammeltoft, and S. Brunak. 2004. Prediction of post-translational glycosylation and phosphorylation of proteins from the amino acid sequence. *Proteomics.* 4:1633–1649.

Boiko, T., M.N. Rasband, S.R. Levinson, J.H. Caldwell, G. Mandel, J.S. Trimmer, and G. Matthews. 2001. Compact myelin dictates the differential targeting of two sodium channel isoforms in the same axon. *Neuron.* 30:91–104.

Boiko, T., A. Van Wart, J.H. Caldwell, S.R. Levinson, J.S. Trimmer, and G. Matthews. 2003. Functional specialization of the axon initial segment by isoform-specific sodium channel targeting. *J. Neurosci.* 23:2306–2313.

Boiko, T., M. Vakulenko, H. Ewers, C.C. Yap, C. Norden, and B. Winckler. 2007. Ankyrin-dependent and -independent mechanisms orchestrate axonal compartmentalization of L1 family members neurofascin and L1/neuron-glia cell adhesion molecule. *J. Neurosci.* 27:590–603.

Bruckner, G., S. Szeoke, S. Pavlica, J. Grosche, and J. Kacza. 2006. Axon initial segment ensheathed by extracellular matrix in perineuronal nets. *Neuroscience.* 138:365–375.

Catimel, B., M. Layton, N. Church, J. Ross, M. Condron, M. Faux, R.J. Simpson, A.W. Burgess, and E.C. Nice. 2006. In situ phosphorylation of immobilized receptors on biosensor surfaces: application to E-cadherin/beta-catenin interactions. *Anal. Biochem.* 357:277–288.

Chung, H.J., Y.N. Jan, and L.Y. Jan. 2006. Polarized axonal surface expression of neuronal KCNQ channels is mediated by multiple signals in the KCNQ2 and KCNQ3 C-terminal domains. *Proc. Natl. Acad. Sci. USA.* 103:8870–8875.

Davis, J.Q., S. Lambert, and V. Bennett. 1996. Molecular composition of the node of Ranvier: identification of ankyrin-binding cell adhesion molecules neurofascin (mucin+/third FNIII domain-) and NrCAM at nodal axon segments. *J. Cell Biol.* 135:1355–1367.

Devaux, J.J., K.A. Kleopa, E.C. Cooper, and S.S. Scherer. 2004. KCNQ2 is a nodal K+ channel. *J. Neurosci.* 24:1236–1244.

Dzhashiashvili, Y., Y. Zhang, J. Galinska, I. Lam, M. Grumet, and J.L. Salzer. 2007. Nodes of Ranvier and axon initial segments are ankyrin G–dependent domains that assemble by distinct mechanisms. *J. Cell Biol.* 177:857–870.

Eshed, Y., K. Feinberg, S. Poliak, H. Sabanay, O. Sarig-Nadir, I. Spiegel, J.R. Bermingham Jr., and E. Peles. 2005. Gliomedin mediates Schwann cell-axon interaction and the molecular assembly of the nodes of Ranvier. *Neuron.* 47:215–229.

Eshed, Y., K. Feinberg, D.J. Carey, and E. Peles. 2007. Secreted gliomedin is a perinodal matrix component of peripheral nerves. *J. Cell Biol.* 177:551–562.

Fache, M.P., A. Moussif, F. Fernandes, P. Giraud, J.J. Garrido, and B. Dargent. 2004. Endocytotic elimination and domain-selective tethering constitute a potential mechanism of protein segregation at the axonal initial segment. *J. Cell Biol.* 166:571–578.

Filhol, O., A. Nueda, V. Martel, D. Gerber-Scokaert, M.J. Benitez, C. Souchier, Y. Saoudi, and C. Cochet. 2003. Live-cell fluorescence imaging reveals the dynamics of protein kinase CK2 individual subunits. *Mol. Cell. Biol.* 23:975–987.

Filhol, O., J.L. Martiel, and C. Cochet. 2004. Protein kinase CK2: a new view of an old molecular complex. *EMBO Rep.* 5:351–355.

Garrido, J.J., F. Fernandes, P. Giraud, I. Mouret, E. Pasqualini, M.P. Fache, F. Jullien, and B. Dargent. 2001. Identification of an axonal determinant in the C-terminus of the sodium channel Na(v)1.2. *EMBO J.* 20:5950–5961.

Garrido, J.J., P. Giraud, E. Carlier, F. Fernandes, A. Moussif, M.P. Fache, D. Debanne, and B. Dargent. 2003. A targeting motif involved in sodium channel clustering at the axonal initial segment. *Science.* 300:2091–2094.

Ghosh, S., F.C. Dorsey, and J.V. Cox. 2002. CK2 constitutively associates with and phosphorylates chicken erythroid ankyrin and regulates its ability to bind to spectrin. *J. Cell Sci.* 115:4107–4115.

Goslin, K., and G. Banker. 1989. Experimental observations on the development of polarity by hippocampal neurons in culture. *J. Cell Biol.* 108:1507–1516.

Hedstrom, K.L., X. Xu, Y. Ogawa, R. Frischknecht, C.I. Seidenbecher, P. Shrager, and M.N. Rasband. 2007. Neurofascin assembles a specialized extracellular matrix at the axon initial segment. *J. Cell Biol.* 178:875–886.

Jenkins, S.M., and V. Bennett. 2001. Ankyrin-G coordinates assembly of the spectrin-based membrane skeleton, voltage-gated sodium channels, and L1 CAMs at Purkinje neuron initial segments. *J. Cell Biol.* 155:739–746.

John, N., H. Krugel, R. Frischknecht, K.H. Smalla, C. Schultz, M.R. Kreutz, E.D. Gundelfinger, and C.I. Seidenbecher. 2006. Brevican-containing perineuronal nets of extracellular matrix in dissociated hippocampal primary cultures. *Mol. Cell. Neurosci.* 31:774–784.

Kole, M.H., S.U. Ilschner, B.M. Kampa, S.R. Williams, P.C. Ruben, and G.J. Stuart. 2008. Action potential generation requires a high sodium channel density in the axon initial segment. *Nat. Neurosci.* 11:178–186.

Kordeli, E., J. Davis, B. Trapp, and V. Bennett. 1990. An isoform of ankyrin is localized at nodes of Ranvier in myelinated axons of central and peripheral nerves. *J. Cell Biol.* 110:1341–1352.

Kordeli, E., S. Lambert, and V. Bennett. 1995. AnkyrinG. A new ankyrin gene with neural-specific isoforms localized at the axonal initial segment and node of Ranvier. *J. Biol. Chem.* 270:2352–2359.

Lambert, S., J.Q. Davis, and V. Bennett. 1997. Morphogenesis of the node of Ranvier: co-clusters of ankyrin and ankyrin-binding integral proteins define early developmental intermediates. *J. Neurosci.* 17:7025–7036.

Lemaillet, G., B. Walker, and S. Lambert. 2003. Identification of a conserved ankyrin-binding motif in the family of sodium channel alpha subunits. *J. Biol. Chem.* 278:27333–27339.

Lim, S.T., D.E. Antonucci, R.H. Scannevin, and J.S. Trimmer. 2000. A novel targeting signal for proximal clustering of the Kv2.1 K+ channel in hippocampal neurons. *Neuron.* 25:385–397.

Lou, J.Y., F. Laezza, B.R. Gerber, M. Xiao, K.A. Yamada, H. Hartmann, A.M. Craig, J.M. Nerbonne, and D.M. Ornitz. 2005. Fibroblast growth factor 14 is an intracellular modulator of voltage-gated sodium channels. *J. Physiol.* 569:179–193.

Martin, P.M., M. Carnaud, G. Garcia del Caño, M. Irondelle, T. Irinopoulou, J.A. Girault, B. Dargent, and L. Goutebroze. 2008. Schwannomin-interacting protein-1 isoform IQCJ-SCHIP-1 is a late component of nodes of Ranvier and axon initial segments. *J. Neurosci.* 28:6111–6117.

Meggio, F., and L.A. Pinna. 2003. One-thousand-and-one substrates of protein kinase CK2? *FASEB J.* 17:349–368.

Misonou, H., M. Menegola, D.P. Mohapatra, L.K. Guy, K.S. Park, and J.S. Trimmer. 2006. Bidirectional activity-dependent regulation of neuronal ion channel phosphorylation. *J. Neurosci.* 26:13505–13514.

Mohler, P.J., I. Rivolta, C. Napolitano, G. LeMaillet, S. Lambert, S.G. Priori, and V. Bennett. 2004. Nav1.5 E1053K mutation causing Brugada syndrome blocks binding to ankyrin-G and expression of Nav1.5 on the surface of cardiomyocytes. *Proc. Natl. Acad. Sci. USA.* 101:17533–17538.

Ogawa, Y., D.P. Schafer, I. Horresh, V. Bar, K. Hales, Y. Yang, K. Susuki, E. Peles, M.C. Stankewich, and M.N. Rasband. 2006. Spectrins and ankyrinB constitute a specialized paranodal cytoskeleton. *J. Neurosci.* 26:5230–5239.

Pan, Z., T. Kao, Z. Horvath, J. Lemos, J.Y. Sul, S.D. Cranstoun, V. Bennett, S.S. Scherer, and E.C. Cooper. 2006. A common ankyrin-G-based mechanism retains KCNQ and NaV channels at electrically active domains of the axon. *J. Neurosci.* 26:2599–2613.

Pagano, M.A., F. Meggio, M. Ruzzene, M. Andrzejewska, Z. Kazimierczuk, and L.A. Pinna. 2004. 2-dimethylamino-4,5,6,7-tetrabromo-1H-benzimidazole: a novel powerful and selective inhibitor of protein kinase CK2. *Biochem. Biophys. Res. Commun.* 321:1040–1044.

Park, K.S., D.P. Mohapatra, H. Misonou, and J.S. Trimmer. 2006. Graded regulation of the Kv2.1 potassium channel by variable phosphorylation. *Science.* 313:976–979.

Politi, C., D. Del Turco, J.M. Sie, P.A. Golinski, I. Tegeder, T. Deller, and C. Schultz. 2007. Accumulation of phosphorylated IkappaBalpha and activated IKK in nodes of Ranvier. *Neuropathol. Appl. Neurobiol.* 313:976–979.

Rich, R.L., and D.G. Myszka. 2007. Survey of the year 2006 commercial optical biosensor literature. *J. Mol. Recognit.* 20:300–366.

Salzer, J.L. 2003. Polarized domains of myelinated axons. *Neuron.* 40:297–318.

Schultz, C., H.G. Konig, D. Del Turco, C. Politi, G.P. Eckert, E. Ghebremedhin, J.H. Prehn, D. Kogel, and T. Deller. 2006. Coincident enrichment of phosphorylated IkappaBalpha, activated IKK, and phosphorylated p65 in the axon initial segment of neurons. *Mol. Cell. Neurosci.* 33:68–80.

Srinivasan, Y., M. Lewallen, and K.J. Angelides. 1992. Mapping the binding site on ankyrin for the voltage-dependent sodium channel from brain. *J. Biol. Chem.* 267:7483–7489.

Published December 8, 2008

Stuart, G., N. Spruston, B. Sakmann, and M. Hausser. 1997. Action potential initiation and backpropagation in neurons of the mammalian CNS. *Trends Neurosci.* 20:125–131.

Theis-Febvre, N., V. Martel, B. Laudet, C. Souchier, D. Grunwald, C. Cochet, and O. Filhol. 2005. Highlighting protein kinase CK2 movement in living cells. *Mol. Cell. Biochem.* 274:15–22.

Wilson, W.D. 2002. Tech.Sight. Analyzing biomolecular interactions. *Science.* 295:2103–2105.

Wittmack, E.K., A.M. Rush, M.J. Craner, M. Goldfarb, S.G. Waxman, and S.D. Dib-Hajj. 2004. Fibroblast growth factor homologous factor 2B: association with Nav1.6 and selective colocalization at nodes of Ranvier of dorsal root axons. *J. Neurosci.* 24:6765–6775.

Yang, Y., Y. Ogawa, K.L. Hedstrom, and M.N. Rasband. 2007. βIV spectrin is recruited to axon initial segments and nodes of Ranvier by ankyrinG. *J. Cell Biol.* 176:509–519.

Zhou, D., S. Lambert, P.L. Malen, S. Carpenter, L.M. Boland, and V. Bennett. 1998. AnkyrinG is required for clustering of voltage-gated Na channels at axon initial segments and for normal action potential firing. *J. Cell Biol.* 143:1295–1304.

Published December 8, 2008

Supplemental Material

JCB

Brechet et al., http://www.jcb.org/cgi/content/full/jcb.200805169/DC1

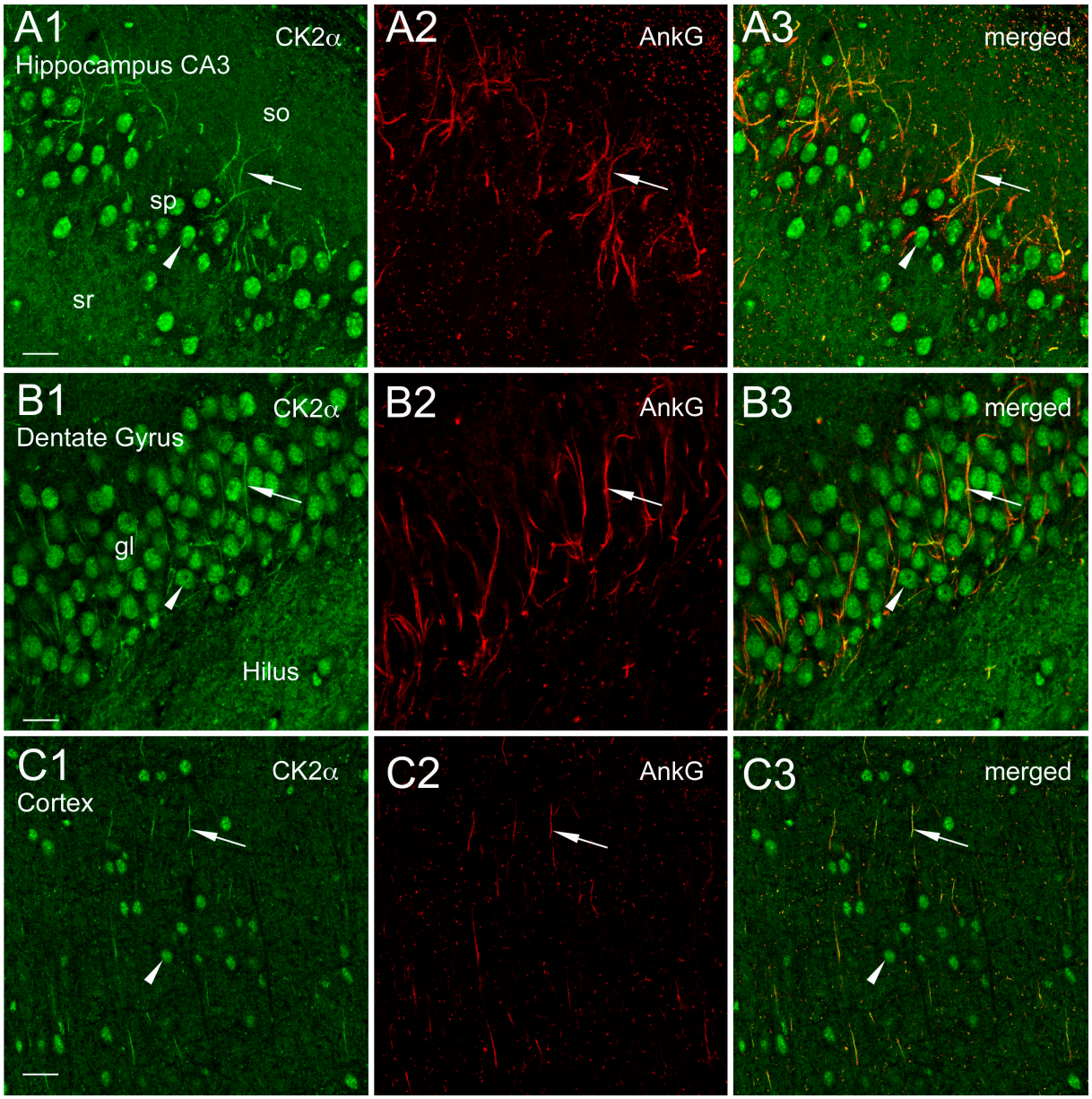

Figure S1. **CK2α is concentrated at axonal initial segments in different rat brain regions.** (A and B) Confocal views showing CK2α immunoreactivity within initial segments (arrows) and nuclei (arrowhead) of neurons in the CA3 area of hippocampus (A1–A3), dentate gyrus (B1–B3), and cortex (layers 4–6, C1–C3). Note that diffuse and light CK2α labeling is visible throughout the neuropil. gl, granular layer; so, stratum; sp, stratum pyramidale; sr, stratum radiatum. Bars: (A) 10 µm; (B) 26.8 µm; (C) 11.37 µm.